A Single ssDNA Aptamer Binding to Mannose-Capped Lipoarabinomannan of Bacillus Calmette−Guérin Enhances Immunoprotective Effect against Tuberculosis

Xiaoming Sun,[†] Qin Pan,[†] Chunhui Yuan,[†] Qilong Wang,[†,§] Xiao-Lei Tang,[†,⊥] Kan Ding,[#] Xiang Zhou,[∥] and Xiao-Lian Zhang*[,†]

[†]State Key Laboratory of Virology and Medical Research Institute, Hubei Province Key Laboratory of Allergy and Immunology and Department of Immunology, Wuhan University School of Medicine, Wuhan 430071, P. R. China

[§]Department of Clinical Oncology, Huai'an First People's Hospital, Nanjing Medical University, Huai'an 223300, China

[⊥]Department of Clinical Laboratory, The Second Hospital of Wuhu, Wuhu 241000, Anhui Province, China

[#]Shanghai Institute of Materia Medica, Shanghai 201203, China

[∥]College of Chemistry and Molecular Sciences, Wuhan University, Wuhan 430072, Hubei Province, China

S Supporting Information

ABSTRACT: Because *Mycobacterium bovis*, termed bacillus Calmette−Guérin (BCG), the only available used tuberculosis (TB) vaccine, retains immunomodulatory properties that limit its protective immunogenicity, there are continuous efforts to identify the immunosuppression mechanism as well as new strategies for improving the immunogenicity of BCG. Here, an ssDNA aptamer "antibody" BM2 specifically bound to the mannose-capped lipoarabinomannan (ManLAM) of BCG was selected. BM2 significantly blocked ManLAM−mannose receptor (MR) binding, triggered ManLAM−CD44 signaling, and enhanced M1 macrophage and Th1 activation via cellular surface CD44 in vitro and in vivo. BM2 enhanced immunoprotective effects of BCG against virulent *Mycobacterium tuberculosis* H37Rv infection in mice and monkeys models. Thus, we report a new mechanism of the interaction between ManLAM and CD44 on macrophages and CD4+ T cells and reveal that ManLAM-binding membrane molecule CD44 is a novel target for the enhancement of BCG immunogenicity, and BM2 has strong potential as an immune enhancer for BCG.
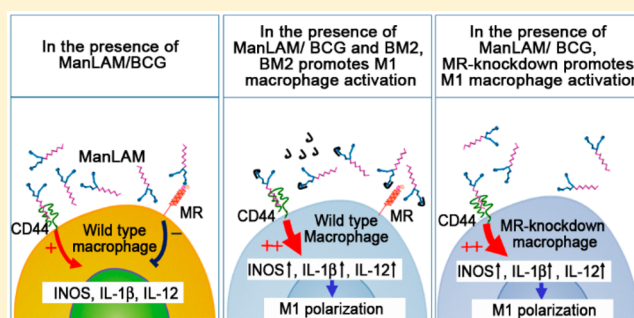
■ INTRODUCTION

Tuberculosis (TB) is the leading cause of death by infectious disease in the world. One-third of the world's population is infected with *Mycobacterium tuberculosis* (*M. tb*). The World Health Organization estimates that approximately 9.6 million new TB cases occur in each year worldwide[1] and 1.5 million deaths occurred worldwide; 3.3% of these cases resulted from multidrug-resistant tuberculosis (MDR-TB) and extensively drug-resistant tuberculosis (XDR-TB) strains and emerged in patients infected with the human immunodeficiency virus.[1−3] An attenuated strain vaccine of *Mycobacterium bovis*, termed bacillus Calmette−Guérin (BCG), the only available used TB vaccine, has been used globally for protection against childhood and disseminated TB. However, its efficacy at protecting against pulmonary TB in adult and aging populations is highly variable.[4,5] The immune response generated by BCG vaccination is incapable of sterilizing the lung after *M. tb* infection, as indicated by the large proportion of individuals with latent TB infection that have received BCG.[6] BCG retains immunosuppressive properties from its pathogenic parent that

limit its protective immunogenicity, which might be related to its limited protective efficacy as a vaccine against TB. However, the immunosuppression mechanism of BCG remains unclear and needs to be further elucidated for the development of new strategies for TB prevention.

Mannose-capped lipoarabinomannan (ManLAM) is a lipoglycan serving as a major cell wall component in both BCG and virulent *M. tb*. For years, ManLAM has been considered a key immunosuppression factor that facilitates virulent *M. tb* immune escape, as evidenced by its interference with host cell recognition, phagosome maturation in macrophages, dendritic cell (DC) maturation, and CD4+ T cell activation in vitro, and ManLAM plays an important role in the pathogenesis of TB.[7−14] Macrophages are the primary host cells of *M. tb*.[7] Increasing evidence has revealed that macrophages are regulated by *M. tb* to allow these bacteria to survive and replicate in cells for an extended period prior to complete
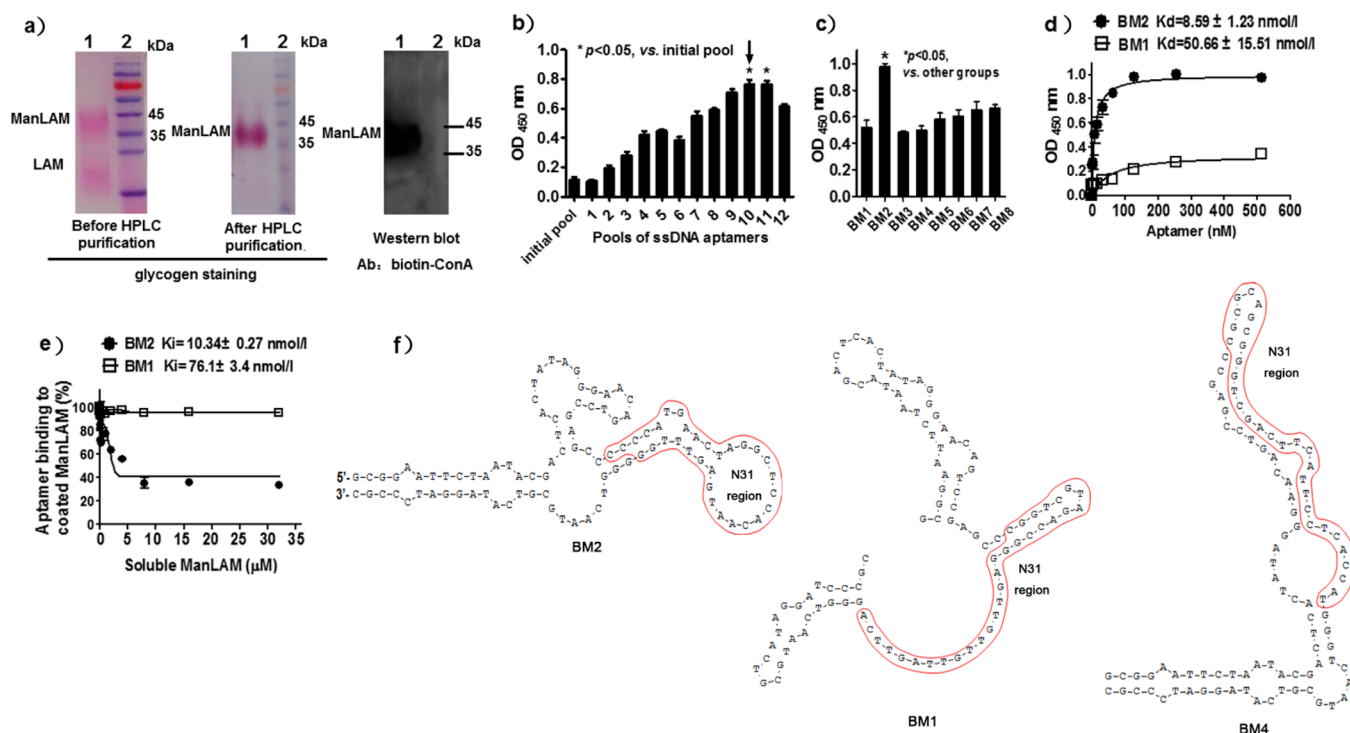
Figure 1. BM2 specifically binds to ManLAM of BCG. (a) ManLAM extracted from BCG was analyzed by SDS−PAGE (visualized by glycogen staining) and Western blot: lane 1, BCG ManLAM; lane 2, marker. (b) After 12 rounds of screening against ManLAM, ssDNA pools from each round were analyzed for their binding to ManLAM by ELONA. Two micromolar aptamers pools (labeled with biotin) were incubated in wells coated with ManLAM (40 μg/mL in PBS). (c) Binding of the single aptamers BM1−BM8 to ManLAM. A 2 μM portion of each single aptamer BM1−BM8 (labeled with biotin) was respectively incubated in wells coated with ManLAM. (d) ELONA analysis of the binding of BM2 to ManLAM. Various concentrations (1, 2, 4, 8, 16, 32, 64, 128, and 512 nM) of BM2 (labeled with biotin) were incubated in wells coated with ManLAM. (e) Soluble ManLAM inhibited BM2 binding to ManLAM coated on the well. The K_d (d) and K_i (e) values were calculated as described previously. (f) Prediction of the secondary structures of BM2, BM1, and BM4. All data in parts b−e are shown as the means ± SEM (n = 3).

activation of protective innate and adaptive immune responses.[8,12,13] However, the mechanisms of ManLAM that are involved with macrophage biology are not completely understood.

Aptamers are single-stranded oligonucleotides with a length of tens of nucleotides and are generated by an in vitro selection process called systematic evolution of ligands by exponential enrichment (SELEX).[15,16] SELEX is an oligonucleotide-based combinatorial library approach that has been extensively used to isolate high-affinity ligands (called aptamers) for a wide variety of targets. Aptamers fold into particular structures to bind to target molecules such as sugars, lipids, proteins, or cells.[17] There are several potential advantages of aptamers over antibodies, such as being of a smaller size, having higher specificity and affinity than antibodies, undergoing easier chemical modifications, having greater stability, being better candidates for cell penetration, and having easier and more economical production methods, and aptamers have been used in numerous investigations as therapeutic or diagnostic tools.[15−17] More importantly, as a lipoglycan, ManLAM is a poor immunogen,[18] and generation of antibody against ManLAM is more difficult than generation of antibody against conventional protein antigens. So we selected aptamer against ManLAM in our study.

Here we used SELEX to generate an ssDNA aptamer BM2 that specifically bound to ManLAM from BCG. We report the discovery of binding of ManLAM of BCG to both CD44 and mannose receptor (MR) on macrophages. Interestingly, BM2 blocked ManLAM−MR binding, triggered ManLAM−CD44

binding, and enhanced macrophage M1 polarization and inflammatory cytokines production via up-regulation of CD44 signaling and down-regulation of MR signaling in macrophages. BM2−ManLAM also stimulated Th1 and Th17 cells via CD44 on CD4^{+} T cells. BM2 significantly enhanced the *M. tb* antigen-presenting activity of macrophages and DCs for naïve CD4^{+} Th1 cell activation. Furthermore, we demonstrate the immune enhancer and immunoadjuvant potentials of BM2 with BCG against virulent *M. tb* H37Rv infection in mice and rhesus monkeys models.

■ RESULTS

High-Affinity ssDNA Aptamers against ManLAM from BCG Are Generated by SELEX. On the basis of the different structures of ManLAM among different *Mycobacteria*, we isolated ManLAM from BCG. The ManLAM from BCG was purified and identified by SDS−PAGE by glycogen staining and Western blot analysis (Figure 1a). Due to the low immunogenicity of ManLAM, we screened aptamer "antibody" against ManLAM by SELEX. To initiate the selection, a random ssDNA library (approximately 10[14] aptamers) was utilized. The ssDNAs (98 mer) that bound to ManLAM coated on the well were selected, and candidate aptamers were enriched at each selection round by PCR amplification. Enrichment of the selection pool through successive rounds of selection was monitored by ELONA (enzyme-linked oligonucleotide assay; see Figure 1b). As shown in Figure 1b, the binding abilities of aptamer pools were increased from round 2, the binding capacity of the 10th and 11th pools was
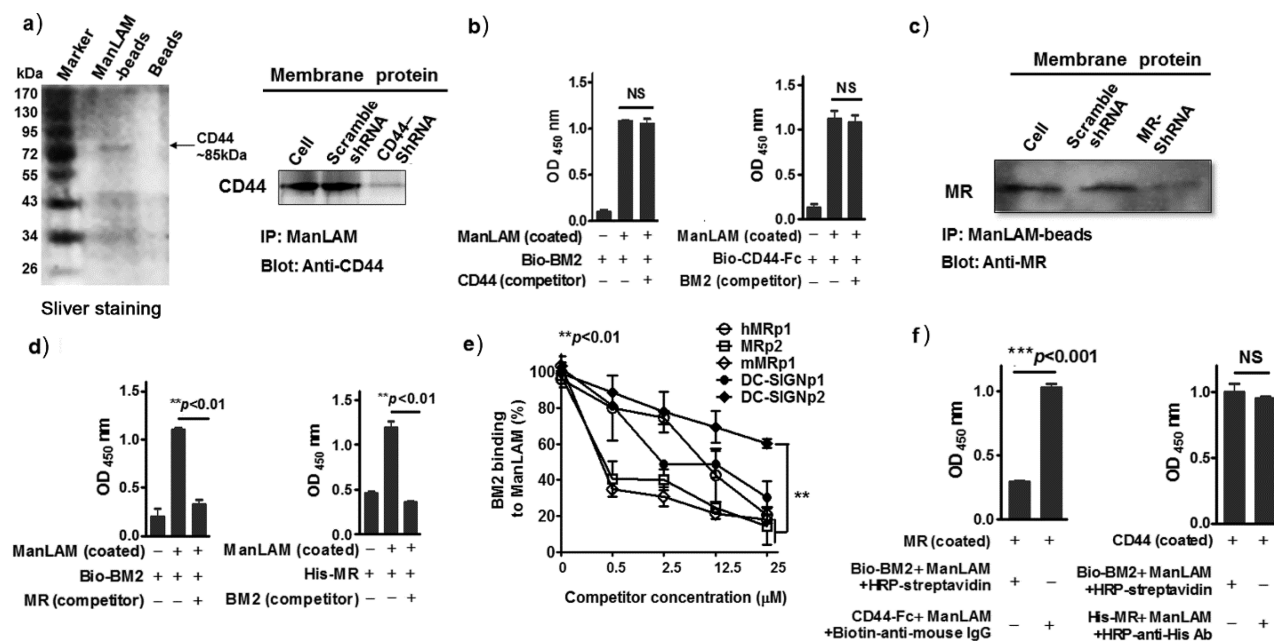
Figure 2. ManLAM binds to both CD44 and MR on macrophages. (a) Left: ManLAM−beads pull-down experiment with membrane extract of mouse peritoneal macrophages, where specific bands were identified by MALDT-TOF-MS. Right: ManLAM pull-down specific bands were identified by immunoblot of CD44. (b) BM2 did not inhibit ManLAM binding to CD44. Left: The ELISA plate was coated with 1 μg/100 μL ManLAM, and 400 nM bio-BM2 and 400 nM CD44-Fc protein were added into ManLAM-coated wells. The binding of bio-BM2 to ManLAM was determined by ELISA. Right: CD44-Fc and BM2 were added into ManLAM-coated wells. The binding of CD44-Fc to ManLAM was determined by ELISA. (c) ManLAM−beads pull-down experiment and immunoblot with anti-MR. (d) Binding of ManLAM to MR was blocked by BM2. Left: The ELISA plate was coated with ManLAM; 400 nM bio-BM2 and 400 nM His-MR protein were added into ManLAM-coated wells. The binding of bio-BM2 to ManLAM was determined by ELISA. Right: BM2 and His-MR were added into ManLAM-coated wells. The binding of His-MR to ManLAM was determined by ELISA. (e) MR peptides inhibited binding of BM2 to ManLAM. (f) The binding sites of ManLAM for MR and CD44 are different. Left: ManLAM (1 μg/100 μL) was incubated with bio-BM2 (400 nM) or CD44-Fc (400 nM) in the MR-coated wells. Right: ManLAM (1 μg/100 μL) was incubated with bio-BM2 (400 nM) or His-MR (400 nM) in the CD44-coated wells. HRP−streptavidin or HRP−anti-His was added, respectively, for color development. All data in parts b and d−f are shown as the means ± SEM (n = 3).

close to saturation, and the affinity of the 12th pool was decreased probably because the 12th pool showed increased specificity but decreased sequence diversity compared with the former pools as the SELEX progressed. Compared with other pools, the 10th ssDNA pool showed the strongest binding ability for ManLAM (Figure 1b). The 10th ssDNA pool was then cloned into pUC19 and individual clones were randomly selected and sequenced. Among these aptamers, BM2 showed the highest ability to bind to ManLAM and BCG (Figure 1c−e), which has a K_d value of 8.59 ± 1.23 nmol/L (Figure 1d). BM1 showed the weakest binding to ManLAM and then was used as irrelevant aptamer control (Figure 1c−e). As shown in Figure 1e, in the presence of about 2.5 μmol/L soluble ManLAM, binding of BM2 to ManLAM coated on the well was reduced to 50% (half-maximal inhibitory concentration, IC$_{50}$ = 2.5 μmol/L). We used GraphPad Prism (GraphPad Software, San Diego, CA) to perform nonlinear curve-fitting analysis. The K_i (the inhibition constant) of BM2 was estimated to be 10.34 ± 0.27 nmol/L (K_i of BM1: 76.1 ± 3.4 nmol/L). Regarding the relationship between K_i and K_d {K_i = IC$_{50}$/(1 + ([L]/K_d)),[19] where [L] is the concentration of the biotin-labeled BM2 used], the evaluated K_d value was in the range between 6.13 and 10.48 nmol/L, which was closely consistent with the calculated K_d of 8.59 ± 1.23 nmol/L, as shown in Figure 1d.

The secondary structures of the selected single ssDNA aptamers BM2, BM1, and BM4 in the 10th round ssDNA pool were predicted by DNAMAN [version 3.2, Lynnon Biosoft; Table S1 of the Supporting Information (SI) and Figure 1f]. In the initial ssDNA library for the SELEX procedure, the central

region (N31) in ssDNAs represented random oligonucleotides based on equal incorporation of A, G, C, and T at each position, resulting in the diversity of ssDNAs. As shown in Figure 1f, the central N31 region of single BM2 aptamer was located at the terminal loop of the stem−loop structure, while the central N31 regions of BM1 and BM4 were located in the helices. These suggest that BM2 might bind to ManLAM via the BM2's terminal loop made up by its central N31 region.

Aptamer BM2 against ManLAM Specifically Binds to ManLAM of BCG in Vitro. To validate the binding specificity of BM2, a BCG ManLAM mutant strain BCGΔ2196 (Figure S1a, SI) that lacked the mannose cap of ManLAM was constructed and identified by SDS−PAGE and gas chromatography (Figure S1b−e, SI). BCG2196 gene encodes the enzyme responsible for the synthesis of ManLAM. When this gene was deleted in BCGΔ2196, the mutant bacteria bound to less concanavalin A (ConA) (a lectin which specifically binds to mannose) compared with BCG according to flow cytometry (FCM) analysis (Figure S2a,b, SI). Then, we used various bacteria, including BCG, BCGΔ2196, *Mycobacterium smegmatis*, *M. tb* H37Rv, *Mycobacterium marinum*, *Mycobacterium intracellulare*, *Mycobacterium avium*, *Staphylococcus aureus*, *Salmonella typhimurium* C5, *Escherichia coli* DH 5α, and *Salmonella typhi* Ty21a, to assess the binding specificity of BM2. As shown in Figure S2c (SI), BM2 bound to much more BCG than to the other bacteria, including BCGΔ2196 and the virulent strain H37Rv. These results suggest that BM2 specifically binds to the mannose caps of BCG ManLAM. Soluble BCG ManLAM acted in a dose-dependent manner to
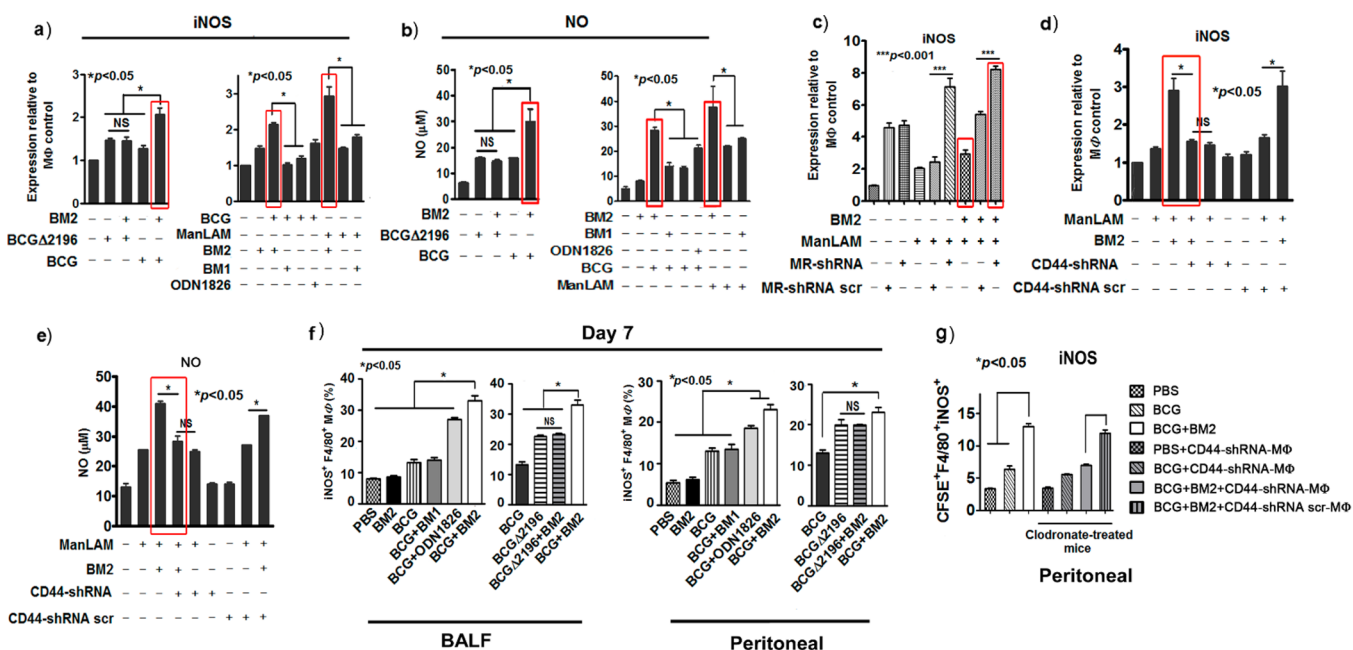
Figure 3. BM2 enhances macrophage M1 polarization. (a) The expression of iNOS of RAW264.7 cells was determined, after being stimulated as indicated for 24 h, by Western blot. The quantification of the iNOS from Western blot image is presented. (b) NO production was determined by nitric oxide assay after being stimulated as indicated for 24 h. (c) BM2 further enhanced iNOS expression in the MR knockdown macrophage cells. RAW264.7 cells were transfected with pSilence1.0-U6-MR-shRNA/MR-shRNA-scr. After 48 h, the cells were stimulated as indicated for 24 h. (d and e) BM2-promoted M1 macrophage polarization was inhibited by CD44−shRNA. RAW264.7 cells were transfected with pSilence1.0-U6-CD44-shRNA/CD44-shRNA-scr. After 48 h, the cells were stimulated as indicated for 24 h. (f) BM2-promoted M1 macrophage polarization in vivo. Mice were immunized as indicated. At day 7 post-immunization, macrophages in broncho-alveolar lavage fluid (BALF) and the peritoneal cavity were collected. The iNOS expression was determined by FCM analysis. (g) BM2-promoted M1 macrophage polarization was inhibited by CD44−shRNA in vivo. The mice were treated with clodronate for macrophage depletion on day 3. On day 0, the mice were immunized as indicated. CFSE-labeled and CD44 knockdown macrophages were adoptively transferred into the mice. The iNOS expression of macrophages on day 7 was analyzed by FCM. The data in parts a−e are shown as the means ± SEM ($n = 3$). The data in parts f and g are shown as the means ± SEM ($n = 6$).

inhibit BM2 binding to BCG bacteria (Figure S2d,e, SI). To validate BM2 sensitivity, the binding of BM2 to various concentrations of BCG was determined (Figure S2f, SI). BM2 showed high sensitivity and enabled the detection of BCG with a broad dynamic range. Even 1×10^4 cfu/100 μL of BCG could be detected by BM2 (Figure S2f, SI).

BM2 Specifically Targets and Binds to BCG in Vivo in a Dose-Dependent Manner. To investigate whether BM2 binds to BCG in vivo, a mixture of the fluorescent dyes AF680-labeled BM2 and Dir-labeled BCG was intravenously (i.v.) injected by tail vein into mice. The BM2−BCG complex was formed prior to injection, and 1 h after injection, BM2 coated on BCG could be detected by ex vivo fluorescent imaging of the lungs (Figure S3a, SI). BM2 alone was not detected by imaging because of its small size (Figure S3a, SI). We did not detect either the control aptamer BM1 binding to BCG or BM2 binding to the control bacteria H37Ra (Figure S3a, SI). BM2 aptamer bound to BCG in a bacterial dose-dependent manner, and even a small amount of BCG (5×10^4 cfu) could be clearly targeted and detected by 5 μM of the BM2 aptamer in mice (Figure S3b, SI).

To determine the stability of the BM2−BCG complex in vivo, mice were injected with a mixture of Dir-BCG and AF680-BM2. The BM2−BCG complex could be detected and remained stable for at least 30 days in vivo (Figure S3c, SI). Then, we determined how long BCG was retained within the lung in vivo. At 1, 10, 20, 30, 60, and 90 days after Dir-BCG injection, AF680-BM2 was injected into the mice 1 h before detection (Figure S3d, SI). BCG could be detected in the lung

(Figure S3d, SI) and spleen (data not shown) even 90 days after BCG injection, indicating that BM2 could track and bind to lung-resident BCG. These data demonstrate that BM2 specifically targets and binds to BCG in vivo. Here, the ssDNA aptamer from the ssDNA−ManLAM complex is more resistant to degradation, probably because the ManLAM molecule in the complex can hinder nucleases binding to and cleaving the ssDNA aptamer.

ManLAM Binds to Both CD44 and MR on Macrophages. To search for potential membrane proteins of macrophages for BCG-ManLAM binding, we performed pull-down assays with ManLAM-coated magnetic beads, followed by mass spectrometry (MS) analysis (left panel in Figure 2a). The SDS−PAGE analysis of membrane extract suggests that the molecular weight of proteins with the highest abundance are between 72 and 95 kDa (Figure S4, SI). Data from the ManLAM−beads pull-down experiment also showed that the 72−95 kDa proteins pulled by ManLAM−beads had the highest abundance (Figure 2a). Therefore, these 72−95 kDa proteins pulled by ManLAM−beads were then analyzed by MS. CD44, a major cell surface receptor, was identified as a novel ManLAM-associated protein.

The binding of ManLAM to CD44 was confirmed by immunoblot (right panel in Figure 2a). Both soluble CD44 protein and BM2 simultaneously bound to ManLAM, and soluble CD44 did not block BM2 binding to ManLAM, suggesting that the binding sites of ManLAM for these two molecules are different (Figure 2b). These also indicate that

BM2 and CD44 do not share an overlapping binding site on ManLAM (Figure 2b).

It has been reported that ManLAM of *M. tb* H37Rv is recognized by MR on macrophages.[20] The binding of BCG−ManLAM to MR was identified by pull-down assays with ManLAM-coated magnetic beads (Figure 2c). Soluble MR protein disrupted the binding of BM2 to ManLAM (left panel in Figure 2d), and BM2 inhibited the binding of MR protein to ManLAM in the competition assay (right panel in Figure 2d). To further confirm the competition between BM2 and MR for binding to ManLAM, MR peptide competitors were used in an ELONA assay (Figure 2e). For competitors, we used the potential binding sites of MR or the dendritic-cell-specific intracellular adhesion molecule 3 (ICAM-3)-grabbing non-integrin (DC-SIGN) as described previously.[21,22] The peptides of mouse mMRp1 [from the cysteine-rich domain of mouse MR(Cys-MR)] and MRp2 (conserved amino acids from a carbohydrate-recognition domain CRD4 for both human and mouse MR) significantly blocked the interaction between BM2 and ManLAM in a dose-dependent manner, while human hMRp1 (from the membrane-distal Cys-MR of human MR) and the control peptides DC-SIGNp1 and DC-SIGNp2 (both from the C-type lectin domains of human DC-SIGN) slightly inhibited BM2 binding (Figure 2e and Table S2, SI). BM2−ManLAM binding was inhibited by approximately 60% in the presence of 0.5 μM of peptide competitors (mMRp1 or MRp2) and approximately 85% in the presence of the highest concentration of peptide competitors (25 μM) from MR (Figure 2e). When biotin-labeled BM2 aptamer bound to ManLAM, it could not bind to MR (Figure 2f). But ManLAM could further bind MR even after ManLAM bound to CD44 (Figure 2f). These results suggest that BM2 and MR may share a partial binding site on ManLAM and that the binding sites of ManLAM for MR and CD44 are different (Figure 2f).

Collectively, these data demonstrate that BM2 interferes with binding of ManLAM to MR but does not inhibit binding of ManLAM to CD44.

BM2−ManLAM Promotes M1 Macrophage Activation and Polarization and Inflammatory Cytokines Production. Activated macrophages are often classified as either classically activated M1 or M2 macrophages.[23] Inducible nitric oxide synthase (iNOS) is a hallmarker for M1 macrophages, and expression of iNOS is necessary for improved resistance to TB.[24] The actions of iNOS and the production of NO correlate well with antimycobacterial defense in murine models of TB infection.[25] To examine the effects of BCG ManLAM and BM2 on the polarization of M1 macrophages, we assessed macrophage polarization in the murine macrophage cell line RAW264.7.

RAW264.7 cells were stimulated by LPS combined with BCG/ManLAM+BM2. BM1 and ODN1826 (oligodeoxynucleotides) were used as ssDNA controls. ODN1826 has been chosen as a broadly nonspecific immune enhancer control.[26] As shown in Figure 3a, BCG/ManLAM alone slightly elevated iNOS expression in RAW264.7 cells. INOS and NO expressions were significantly up-regulated in the presence of BCG+BM2 or ManLAM+BM2 compared with the BCG/ManLAM, BCG+BM1, or ManLAM+BM1 and BCGΔ2196+BM2 groups (Figure 3a−c, Figure S5a, SI). There was no significant difference in iNOS and NO expressions between the BCGΔ2196 and BCGΔ2196+BM2 groups (Figure 3a−c). These results suggest that BM2 binding to ManLAM elevates iNOS and NO productions of macro-

phages. Additionally, BM2 may induce iNOS and NO more efficiently than ODN1826 (Figure 3a,b). No significant difference of arginase-1 (Arg-1) expression was observed between the ManLAM+BM2 group and other groups (data not shown).

M1 macrophages often increase production of inflammatory cytokines such as IL-12 and IL-1β.[27] IL-1 confers host resistance to *M. tb* through the induction of eicosanoids that limit excessive type I interferon (IFN) production and foster bacterial containment.[28] In contrast, M2 macrophages often produce anti-inflammatory cytokine IL-10.[29] Cytokine production caused by BM2 in RAW264.7 cells was determined by ELISA. As shown in Figure S5b−d (SI), BM2 enhanced IL-12p70 (Figure S5b, SI) and IL-1β (Figure S5c, SI) cytokines production but decreased IL-10 (Figure S5d, SI) production in the BCG+BM2 or ManLAM+BM2 group.

BM2−ManLAM Activates M1 Macrophage and Enhances the Antigen Presentation Ability of Macrophage. Next, we further investigated the possible roles of CD44 and MR in BM2-induced M1 polarization. When MR was silenced in macrophages by MR−shRNA, we found that BM2 further increased iNOS expression in the ManLAM-treated and MR−shRNA-transfected RAW264.7 cells compared with the shRNA scramble (shRNA-scr) control group (eighth and ninth columns from left to right in Figures 3c and S6a, SI). There is no difference in iNOS expressions of macrophage between the MR−shRNA group and MR−shRNA scr group in the absence of ManLAM binding and stimulation (second and third columns from left to right, Figure 3c). These suggest that ManLAM stimulates iNOS expression when MR is silenced and indicates that ManLAM negatively regulates iNOS expression via MR.

Considering ManLAM binding to CD44 (Figure 2a), we assessed the effects of ManLAM−CD44 binding on the macrophages. When CD44 was silenced in macrophages by CD44−shRNA, iNOS expression (Figure 3d and Figure S6b) and NO production (Figure 3e) were significantly decreased in the presence of BM2 plus ManLAM compared with the CD44−shRNA-scr group. These data suggest that the interaction of BCG−ManLAM with BM2 triggered ManLAM−CD44 signaling and enhanced M1 macrophage activation via up-regulation of CD44 and down-regulation of MR signaling, as evidenced by positively regulating the iNOS and NO expressions.

We further verified BM2-enhanced M1 macrophage activation and polarization in vivo. Mice were immunized with BM2+BCG. At day 7 and day 30 post-immunization, FCM analysis showed that iNOS expressions of macrophages in both BALF and peritoneal cavity were significantly increased in the BCG+BM2 group compared with other groups on day 7 (Figure 3f) and day 30 (Figure S6c, SI).

Further, CD44−shRNA-transfected macrophages labeled by carboxyfluorescein diacetate succinimidyl ester (CFSE) dye were transferred into macrophage-depleted mice, as shown in Figure 3g. The polarization of murine macrophages was evaluated 7 days after adoptive transfer (Figure 3g). Consistent with in vitro results, much higher expression of iNOS in CFSE$^+$F4/80$^+$ macrophages was observed in the BCG+BM2 treated group compared with the BCG group (Figure 3g). However, adoptive transferring of CD44−shRNA−macrophages caused much lower iNOS expression of CFSE$^+$F4/80$^+$ macrophages in the BCG+BM2-treated group than those of the CD44−shRNA-scr-treated group (Figure 3g).
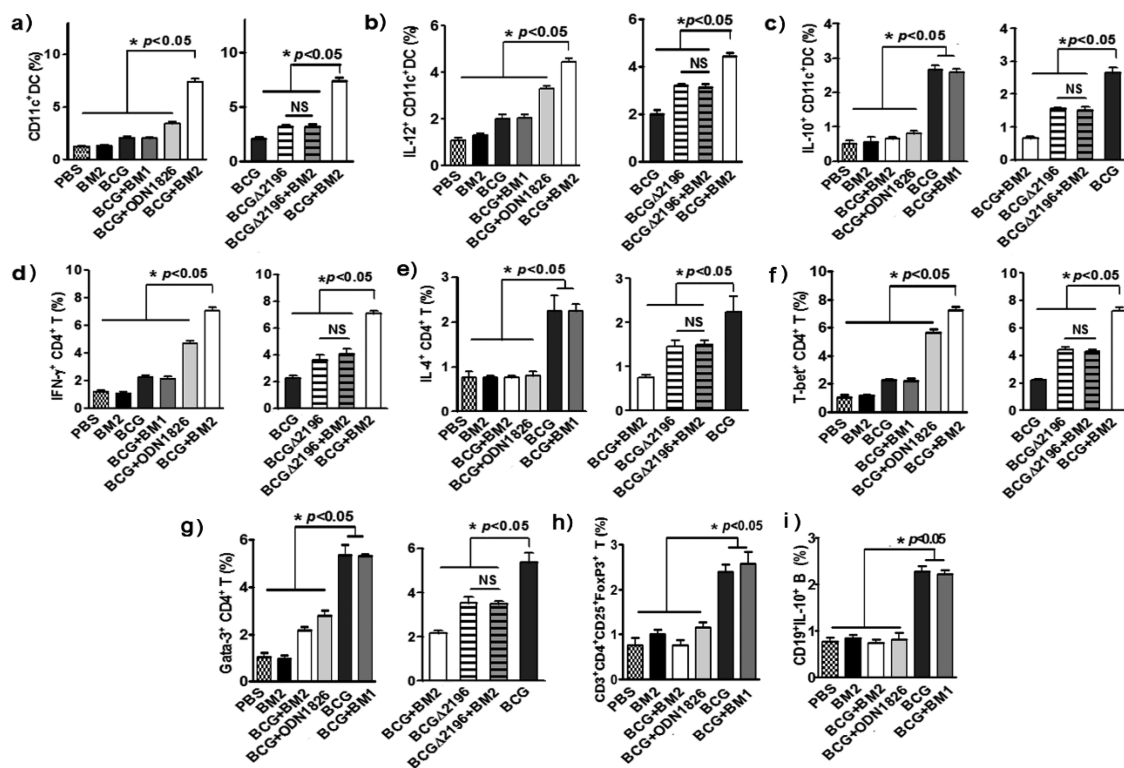
Figure 4. BM2 promotes Th1 cell polarization and enhances immunogenicity of BCG in mice. At day 0, mice were immunized as indicated. At day 30 post-vaccination, mice were sacrificed and immune cells from lymph were prepared for FCM analysis. (a) BM2 improved the homing of DCs to lymph nodes upon BCG vaccination. CD11c$^+$ DCs in the lymph nodes were determined by FCM. (b) BM2 enhanced the IL-12 production but (c) decreased IL-10 production by CD11c$^+$ DCs in lymph nodes upon BCG vaccination. (d) BM2 enhanced the IFN-γ production but (e) decreased IL-4 production by CD4$^+$ T cells upon BCG vaccination. (f) BM2 enhanced the T-bet but (g) decreased Gata-3 expression in CD4$^+$ T cells upon BCG vaccination. The regulatory cells, (h) Tregs and (i) IL-10 producing B cells (Bregs) were decreased in BCG+BM2. All data are shown as the means $\pm$ SEM ($n = 6$).

Moreover, the expressions of CD44, MHC-II, and costimulatory molecule CD83 on RAW264.7 cells were upregulated by ManLAM/BCG in the presence of BM2 but not BM1 (Figure S7a,b, SI). Blockage of ManLAM binding to CD44 by anti-CD44 antibody virtually eliminated the BM2-induced enhancement of MHC-II and the costimulatory molecule CD83 on ManLAM-treated RAW264.7 cells (Figure S7b, SI).

All these data suggest that BM2 may activate M1 macrophage in vitro (Figure 3d,e) and in vivo (Figure 3g) and enhance the antigen presentation ability of macrophages, as evidenced by increased MHC-II, costimulatory molecule expression as well as increased iNOS and IL-12/IL-1β expression and decreased IL-10 expression via BM2−ManLAM−CD44 interaction.

BM2−ManLAM Stimulates Th1 and Th17 Cells via CD44 on CD4$^+$ T Cell in Vitro. CD44 was previously reported to be expressed on T cells and involved in cellular functions such as lymphocyte activation and recirculation.[30] We further examined the effects of ManLAM−CD44 binding on T cell activation in the presence of BM2. CD4$^+$ naïve T cells were activated with anti-CD3 antibody and anti-CD28 antibody in the presence of ManLAM (with or without BM2). We found that ManLAM and/or BM2 did not change the surface CD44 expression level of CD3$^+$CD4$^+$ T cells (Figure S8a, SI). In the presence of BM2, ManLAM significantly enhanced the intracellular INF-γ and IL-17A productions and decreased IL-10 production of CD3$^+$CD4$^+$ T cells (Figure S8b,d,e, SI). Compared with anti-CD44 isotype group, addition of anti-

CD44 alone caused reduction of the IFN-γ and IL-17A production by CD4$^+$ T cells (third column from left to right vs fourth column, Figure S8b,d, SI). However, addition of anti-CD44 caused further reduction of the IFN-γ and IL-17A production by the CD4$^+$ T cells treated with ManLAM and BM2 (sixth column from left to right vs seventh column, Figure S8b,d, SI). ManLAM alone slightly down-regulated the productions of intracellular IFN-γ, IL-4, and IL-17A cytokines but increased intracellular IL-10 production of CD3$^+$CD4$^+$ T cells (Figure S8b−e, SI), which indicate that ManLAM alone has immunosuppressive effects on T cells. IL-4 production was not changed when the cells were subject to BM2+ManLAM treatment (Figure S8c, SI). When anti-CD44 antibody was used to block the ManLAM−CD44 binding, the IL-10 reduction caused by BM2 was not affected by anti-CD44 (Figure S8e, SI). IFN-γ secretion is a hallmark of Th1 cells, while IL-4 is secreted mainly from activated Th2 cells. IL-17 secretion is a hallmark of Th17 cells. Elicitation of Th1 and Th17 immunity contributes to *M. tb* elimination in host.[31] Our data demonstrate that BM2−ManLAM stimulates Th1 and Th17 cells via CD44 on CD4$^+$ T cells in vitro.

BM2 Enhances Immunogenicity of BCG in Mice. Our data (Figure 3) has shown that BM2 activates M1 macrophage in vitro and in vivo. We further evaluated the BM2 effects on DCs and Th1 cells in BCG-immunized mice. Balb/c mice were immunized with BCG+BM2 once. At day 30 post-immunization, immune cells from lymph nodes were prepared and assessed for their response to *M. tb* antigens (heat-inactivated bacteria). We found more DCs in the lymph nodes from the
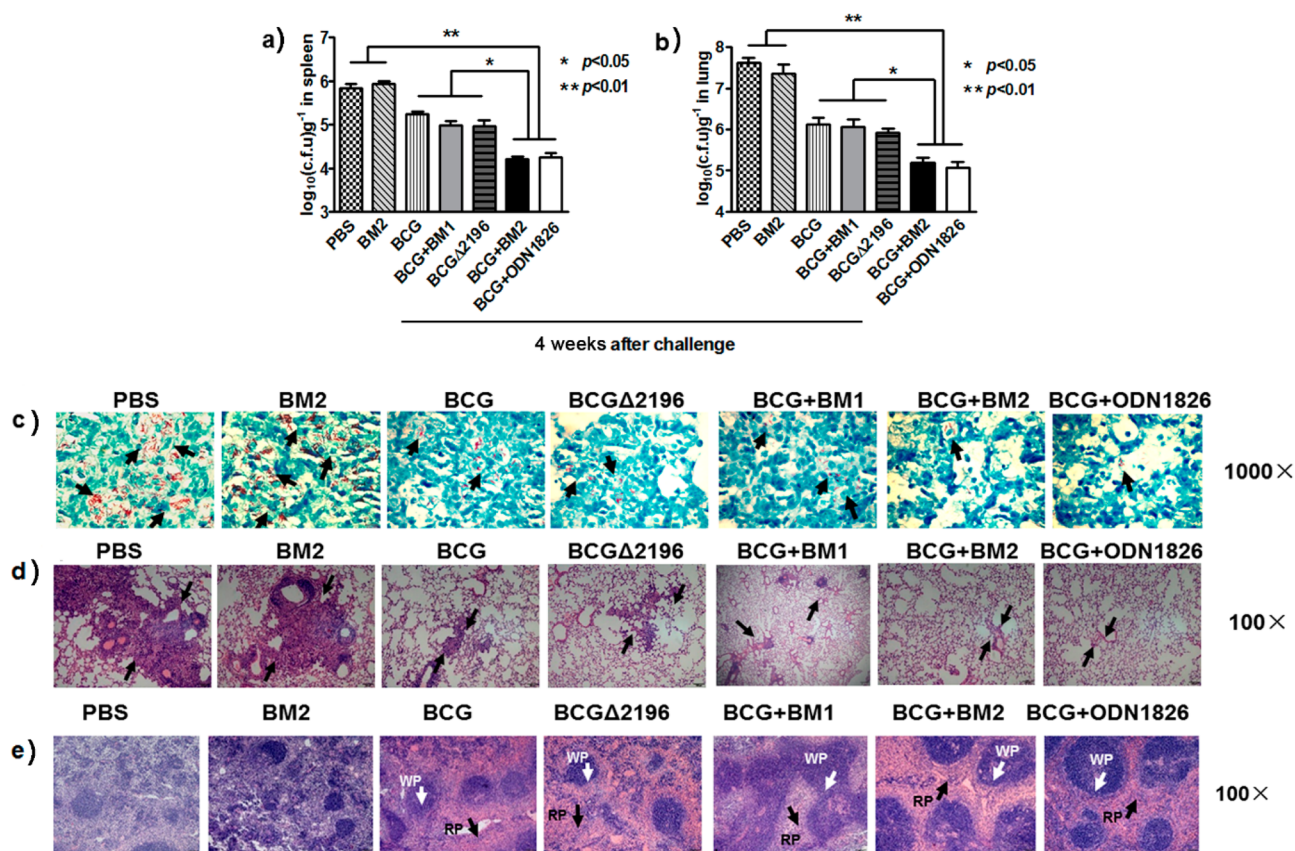
Figure 5. BM2 increases protective efficiency of BCG against *M. tb* H37Rv infection in mice. On week −4, BALB/c mice were vaccinated with BCG + BM2/BM1/ODN1826, BCG, or BCGΔ2196 once. On week 0, the mice were aerogenically challenged with *M. tb* H37Rv (100 cfu per mouse). On week 4, the mice were sacrificed, and *M. tb* cfu assay, acid-fast stain analysis, and histopathological analyses were performed. *M. tb* cfu assay in spleens (a) and in lungs (b). All data for parts a and b are shown as the means ± SEM ($n = 6$). (c) The lung tissue sections were analyzed with Ziehl−Neelsen acid-fast stain (1000×). Black arrows represent the bacteria. Lung (d) and spleen (e) tissue sections were stained with hematoxylin and eosin (H&E) and evaluated by light microscopy (100×). The arrows indicate the pulmonary lesions (d) and the WP/RP in spleen tissue sections (e).

BCG+BM2 group compared with other groups, suggesting that immunization with BCG+BM2 recruited much more CD11$^+$ DCs to migrate into the lymph nodes by day 30 after immunization (Figure 4a). As shown in Figure 4, DCs in the BCG+BM2 group enhanced IL-12 production (Figure 4b) but decreased IL-10 production (Figure 4c) by day 30 after immunization. This indicates that BM2 may also activate DCs and enhance the antigen presentation ability of DCs in BCG-immunized mice.

We also determined that IFN-γ-producing CD4$^+$ T cells increased best in the BCG+BM2 group compared with other groups (Figure 4d). However, IL-4-producing CD4$^+$ T cells from the spleen decreased in the BCG+BM2 group compared with the BCG, BCG+BM1, or BCGΔ2196+BM2 groups (Figure 4e). Consistent with the cytokine production, the expression of Th1 transcription factor T-bet (Figure 4f) in splenic CD4$^+$ T cells increased, but the Gata-3 expression of Th2 transcription factor (Figure 4g) decreased in the BCG+BM2 group. These results indicated that when combined with BM2, the BCG vaccine polarized T cell response toward a Th1 cellular immune response by the enhanced IFN-γ expression. No significant difference was observed between the BCGΔ2196 and BCGΔ2196+BM2 groups (Figure 4a−g). In addition, Treg and Breg cells were decreased in the BCG+BM2 group compared with the BCG+BM1 and BCG groups (Figure 4h,i). These data suggested that BCG+BM2 vaccination significantly

enhanced Th1-type immune response and induced stronger immunogenicity of BCG.

BM2 Increases Protective Efficiency of BCG against *M. tb* H37Rv Infection in Mice and Monkeys. To evaluate the effects of BM2 on BCG-immunized mice during *M. tb* infection, the immunized mice were challenged with *M. tb* H37Rv by aerosol. We used ODN1826 as the positive control adjuvant of BCG. ODN1826 is a CpG oligodeoxynucleotide that is a toll-like receptor (TLR) 9 ligand, induces the Th1-type immune response, and is widely used as a nonspecific effective immune enhancer and vaccine adjuvant.[26] When we administered BCG/BCG+BM2 (0.5 nmol BM2 per mouse) or BCG +ODN1826 (10 nmol ODN1826 per mouse) once into each mouse, we found that immunization with BCG+BM2 or BCG +ODN1826 significantly reduced *M. tb* H37Rv colony-forming units (cfu) in mouse lung (Figure 5a) and spleen (Figure 5b) after 30 days of infection. Acid-fast stain analysis also showed few bacteria in the BCG+BM2 groups (Figure 5c). Compared with the BCG+BM1 and BCG groups, histopathological analysis of lung alveolar tissue from the BCG+BM2 group showed that the numbers and size of granulomas were smaller, and the lung tissue was mostly intact with only mild signs of alveolitis, a small amount of lymphocyte infiltration, and a few red blood cells present in connective tissue (Figure 5d). Necrotic and proliferative granulomas were observed in the PBS and BM2 control groups (Figure 5d). The lymphoid white

pulp (WP) and red pulp (RP) in spleen tissues were more clearly evident in the BCG+BM2 group compared with the PBS and BM2 control groups (Figure 5e).

M. tb pathogenesis and the ability of host immunity to challenge infection in rhesus monkeys closely mimics the symptoms of human TB disease.[32] Therefore, BM2 was assessed in a rhesus monkey model of TB. Because of the expense, a total of eight rhesus monkeys (RM) were used in three groups (PBS, BCG, and BCG+BM2 groups), and we did not use statistical analysis to compare data from these three groups. Prior to infection with *M. tb* H37Rv, 5 weeks after immunization, IFN-γ production by peripheral blood mononuclear cells (PBMCs) in the BCG+BM2 group was greatly increased compared with the PBS and BCG groups (Figure S9a, SI). At week 6, the results of purified protein derivative (PPD) skin test demonstrated that all monkeys were successfully infected with virulent *M. tb* H37Rv (Figure S9b and Table S3, SI). At week 17 after infection, BCG+BM2 immunization most remarkably reduced the *M. tb* H37Rv cfu bacterial load in lungs compared with the BCG group and PBS control treatment (Figure S9c, SI). Results from computer tomography (CT) detection for pulmonary tuberculosis demonstrated that the number of granulomas was fewer and size of lung lesions was smaller in the BCG+BM2 group compare with the PBS group (Figure S9d, SI). Lung histological analysis (Figure S9e, SI) showed pulmonary granulomatous lesions with leukocyte infiltration in the PBS group. No granulomatous lesions were found in the pulmonary parenchyma of either the BCG or BCG+BM2 group (Figure S9e, SI). Together, these data indicated that vaccination with BCG+BM2 induced greater protective anti-TB immunity than immunization with BCG alone in mice and monkeys.

■ DISCUSSION

Aptamers have enormous potential as therapeutics or diagnostic tools because they exhibit high affinity and specificity toward recognition targets and inhibit their functions with minimal or no harmful side effects.[32,33] A targeted anti-VEGF RNA aptamer (Macugen), the first aptamer therapeutic, was FDA approved in 2005, and a number of novel aptamer-based therapeutics are currently undergoing clinical trials.[34] Our selected ssDNA aptamer BM2 was demonstrated to be safe with low toxicity based on in vitro and in vivo toxicity analyses (Figure S10a–g, SI).

ManLAM antibody treatment and anti-ManLAM aptamer treatment decrease bacterial loads and dissemination, prolong survival, and get better disease outcome in animal models of TB.[22,35] It has been reported that ManLAM of *M. tb* H37Rv inhibits phagosome maturation in macrophages and acts as modulators of DC and Th1, while LAM lacking mannose caps does not exhibit this activity.[13,36–38] BCG mutants alone, which have a ManLAM-capping deficiency, may not be sufficient to improve the immunogenicity of BCG.[39,40] Our present study demonstrated that BCGΔ2196 alone was much less effective at improving M1 macrophage and Th1 polarization compared with BM2+BCG, which suggests that BM2 is much better for blocking the immunosuppressive effects of BCG mediated by ManLAM than BCGΔ2196 alone.

It has been reported that *M. tb* enhances its survival in macrophages by suppressing immune responses in part through activation of peroxisome proliferator-activated receptor γ (PPARγ) through a macrophage MR-dependent pathway induced by *M. tb* cell wall ManLAM.[20] PPARγ knockdown in

human macrophages enhances TNF production and controls the intracellular growth of *M. tb*.[20] Our data showed that BM2 alone specifically interfered with binding of ManLAM to MR and reduction of iNOS expression (Figure. 3), which might lead to reduced MR-PPARγ signaling and contribute to the control of the intracellular growth of virulent *M. tb* H37Rv.

There are multiple bands visible in the pull-down experiment, and CD44 is not the only band in this SDS−PAGE gel, suggesting there are other proteins involved (Figure 2a). It has been reported that ManLAM can be recognized by several receptors, including toll-like receptors (TLR2 and TLR4), MR, DC-SIGN, sphingosine-1-phosphate receptor 1 (S1P1), and CD1d, as well as dectin-2.[37,41−49] In further studies, we will investigate the effects of binding of ManLAM and various receptors in macrophages.

BM2 alone plays two roles by blocking binding of ManLAM to MR and by inhibiting down-regulation of iNOS signaling (Figure 2), as well as by promoting the interaction of ManLAM−CD44, CD44 expression, and up-regulation of iNOS signaling in macrophages. BM2 did not inhibit binding of ManLAM to CD44 (Figure 2). We reveal a novel mechanism in which macrophage M1 polarization is triggered by ManLAM−CD44 binding and ManLAM aptamer BM2 enhances macrophage M1 polarization via up-regulation of CD44 and down-regulation of MR signaling and enhances immunoprotective effects of BCG in both mouse and monkey models. Further, BM2 maximally induces iNOS expression of M1 macrophages in MR-knockdown cells (Figure 3). In the mouse model of vaccination and *M. tb* challenge, BM2 promotes M1 polarization, migration of DCs to lymph nodes, and Th1-type immune response in vivo (Figures 3 and 4). These contribute to the increase protective efficiency of BCG against *M. tb* H37Rv infection (Figure 5a−e). Our results indicate that BCG ManLAM and CD44 are new putative molecular targets for the improvement of BCG immunogenicity and immunoproective effects.

After subcutaneous injection, BM2−BCG will be taken up mainly by antigen-presenting cells, such as DCs and macrophages. In our previously published work, we have demonstrated that enhancement of the *M. tb*-antigen-presenting activity of DCs leads to promotion of naïve CD4^{+} T cell activation by using ssDNA aptamer targeting ManLAM purified from virulent strain *M. tb* H37Rv.[22] In the current study, we used anti-CD3 and anti-CD28 antibodies to activate CD4^{+} T cells in vitro and assessed the effects of BM2−ManLAM on the cytokine production of CD4^{+} T cells (Figure S8, SI). Our data indicate that ManLAM−BM2 complex might directly induce the Th1 and Th17 polarization of activated CD4^{+} T cells via CD44. It was also reported that *M. tb* H37Rv ManLAM's interactions with host cell receptors and membranes result in altered cellular signaling and responses. This is thought to be achieved through a steric inhibition mechanism or through direct binding of host proteins to the acyl tails of ManLAM itself, which resemble mammalian phosphatidylinositol-3,4,5-trisphosphate.[37] The molecular mechanisms of ManLAM of different mycobacteria on CD4^{+}T cells might be via different signaling pathways.

Moreover, we assessed the mRNA expressions of TLRs in BM2-treated mouse peritoneal macrophages. As shown in Figure S11 (SI), addition of BM2 alone significantly enhance the mRNA expressions of TLRs in BM2-treated peritoneal macrophages. However, compared with the macrophages treated with TLR agonists, BM2-alone treatment caused a

much lower degree of enhancement of mRNA expressions of TLRs. These results indicate that BM2 alone might stimulate the macrophages at low levels.

Additionally, BCG has been shown to be effective immunotherapy for patients with high-risk bladder tumors, particularly for carcinoma in situ.[50,51] We respect that BM2 combined with BCG might be better used than BCG alone in bladder cancer therapy, as well.

CONCLUSION

We used SELEX to generate an ssDNA aptamer BM2 that specifically bound to ManLAM from BCG. We report the discovery of ManLAM of BCG binding to both CD44 and MR on macrophages. BM2 blocked ManLAM−MR binding, triggered ManLAM−CD44 binding, and enhanced macrophage M1 polarization and inflammatory cytokines production via up-regulation of CD44 signaling and down-regulation of MR signaling in macrophages. BM2−ManLAM also stimulated Th1 and Th17 cells via CD44 on CD4^{+} T cells. BM2 significantly enhanced the *M. tb*-antigen-presenting activity of macrophages and DCs for naïve CD4^{+} Th1 cell activation. Here, we demonstrate the immune-enhancing and immunoadjuvant potentials of BM2 with BCG against virulent *M. tb* H37Rv infection in mice and rhesus monkeys models.

ASSOCIATED CONTENT

ⓈSupporting Information

The Supporting Information is available free of charge on the ACS Publications website at DOI: 10.1021/jacs.6b05357.

> Data of SELEX procedures and ssDNA aptamer characterization, BCGΔ2196 construction and identification, cytokine production and expression of costimulatory molecules on ManLAM-treated macrophages, cytokine production of ManLAM-treated CD4^{+} T cells, results of PPD skin test and CT detection of pulmonary tuberculosis in rhesus monkeys, and toxicity analysis of BM2 (PDF)

AUTHOR INFORMATION

Corresponding Author
*zhangxiaolian@whu.edu.cn

Author Contributions
X.S. and Q.P. contributed equally to this work.

Notes
The authors declare no competing financial interest.

ACKNOWLEDGMENTS

REFERENCES

(1) World Health Organization. *Global Tuberculosis Report 2015*, 20th ed.; World Health Organization: Geneva, 2015.

(2) Svenson, S.; Kallenius, G.; Pawlowski, A.; Hamasur, B. *Hum. Vaccines* **2010**, *6*, 309.

(3) Manjelievskaia, J.; Erck, D.; Piracha, S.; Schrager, L. *Trans. R. Soc. Trop. Med. Hyg.* **2016**, *110*, 186.

(4) Monkongdee, P.; McCarthy, K. D.; Cain, K. P.; Tasaneeyapan, T.; Dung, N. H.; Lan, N. T. N.; Yen, N. T. B.; Teeratakulpisarn, N.; Udomsantisuk, N.; Heilig, C.; Varma, J. K. *Am. J. Respir. Crit. Care Med.* **2009**, *180*, 903.

(5) Colditz, G. A.; Brewer, T. F.; Berkey, C. S.; Wilson, M. E.; Burdick, E.; Fineberg, H. V.; Mosteller, F. *JAMA, J. Am. Med Assoc.* **1994**, *271*, 698.

(6) Moliva, J. I.; Turner, J.; Torrelles, J. B. *Vaccine* **2015**, *33*, 5035.

(7) Briken, V.; Porcelli, S. A.; Besra, G. S.; Kremer, L. *Mol. Microbiol.* **2004**, *53*, 391.

(8) Fratti, R. A.; Chua, J.; Vergne, I.; Deretic, V. *Proc. Natl. Acad. Sci. U. S. A.* **2003**, *100*, 5437.

(9) Maeda, N.; Nigou, J.; Herrmann, J. L.; Jackson, M.; Amara, A.; Lagrange, P. H.; Puzo, G.; Gicquel, B.; Neyrolles, O. *J. Biol. Chem.* **2003**, *278*, 5513.

(10) Nigou, J.; Zelle-Rieser, C.; Gilleron, M.; Thurnher, M.; Puzo, G. *J. Immunol.* **2001**, *166*, 7477.

(11) Nigou, J.; Gilleron, M.; Puzo, G. *Biochimie* **2003**, *85*, 153.

(12) Sibley, L. D.; Hunter, S. W.; Brennan, P. J.; Krahenbuhl, J. L. *Infect. Immun.* **1988**, *56*, 1232.

(13) Welin, A.; Winberg, M. E.; Abdalla, H.; Sarndahl, E.; Rasmusson, B.; Stendahl, O.; Lerm, M. *Infection and immunity* **2008**, *76*, 2882.

(14) Mahon, R. N.; Sande, O. J.; Rojas, R. E.; Levine, A. D.; Harding, C. V.; Boom, W. H. *Cell. Immunol.* **2012**, *275*, 98.

(15) Ellington, A. D.; Szostak, J. W. *Nature* **1990**, *346*, 818.

(16) Tuerk, C.; Gold, L. *Science* **1990**, *249*, 505.

(17) Mayer, G. *Angew. Chem., Int. Ed.* **2009**, *48*, 2672.

(18) Hamasur, B.; Kallenius, G.; Svenson, S. B. *Vaccine* **1999**, *17*, 2853.

(19) Krohn, K. A.; Link, J. M. *Nucl. Med. Biol.* **2003**, *30*, 819.

(20) Rajaram, M. V.; Brooks, M. N.; Morris, J. D.; Torrelles, J. B.; Azad, A. K.; Schlesinger, L. S. *J. Immunol.* **2010**, *185*, 929.

(21) Torrelles, J. B.; Azad, A. K.; Schlesinger, L. S. *J. Immunol.* **2006**, *177*, 1805.

(22) Pan, Q.; Wang, Q.; Sun, X.; Xia, X.; Wu, S.; Luo, F.; Zhang, X. L. *Mol. Ther.* **2014**, *22*, 940.

(23) Mattila, J. T.; Ojo, O. O.; Kepka-Lenhart, D.; Marino, S.; Kim, J. H.; Eum, S. Y.; Via, L. E.; Barry, C. E., 3rd; Klein, E.; Kirschner, D. E.; Morris, S. M., Jr.; Lin, P. L.; Flynn, J. L. *J. Immunol.* **2013**, *191*, 773.

(24) MacMicking, J. D.; North, R. J.; LaCourse, R.; Mudgett, J. S.; Shah, S. K.; Nathan, C. F. *Proc. Natl. Acad. Sci. U. S. A.* **1997**, *94*, 5243.

(25) Scanga, C. A.; Mohan, V. P.; Tanaka, K.; Alland, D.; Flynn, J. L.; Chan, J. *Infection and immunity* **2001**, *69*, 7711.

(26) Freidag, B. L.; Melton, G. B.; Collins, F.; Klinman, D. M.; Cheever, A.; Stobie, L.; Suen, W.; Seder, R. A. *Infection and immunity* **2000**, *68*, 2948.

(27) Benoit, M.; Desnues, B.; Mege, J. L. *J. Immunol.* **2008**, *181*, 3733.

(28) Mayer-Barber, K. D.; Andrade, B. B.; Oland, S. D.; Amaral, E. P.; Barber, D. L.; Gonzales, J.; Derrick, S. C.; Shi, R.; Kumar, N. P.; Wei, W.; Yuan, X.; Zhang, G.; Cai, Y.; Babu, S.; Catalfamo, M.; Salazar, A. M.; Via, L. E.; Barry, C. E., III; Sher, A. *Nature* **2014**, *511*, 99.

(29) Bohlson, S. S.; O'Conner, S. D.; Hulsebus, H. J.; Ho, M. M.; Fraser, D. A. *Front. Immunol.* **2014**, *5*, 402.

(30) Cao, H.; Heazlewood, S. Y.; Williams, B.; Cardozo, D.; Nigro, J.; Oteiza, A.; Nilsson, S. K. *Haematologica* **2016**, *101*, 26.

(31) Rai, P. K.; Chodisetti, S. B.; Nadeem, S.; Maurya, S. K.; Gowthaman, U.; Zeng, W.; Janmeja, A. K.; Jackson, D. C.; Agrewala, J. N. *Sci. Rep.* **2016**, *6*, 23917.

(32) Okada, M.; Kita, Y.; Nakajima, T.; Kanamaru, N.; Hashimoto, S.; Nagasawa, T.; Kaneda, Y.; Yoshida, S.; Nishida, Y.; Fukamizu, R.;

Tsunai, Y.; Inoue, R.; Nakatani, H.; Namie, Y.; Yamada, J.; Takao, K.; Asai, R.; Asaki, R.; Matsumoto, M.; McMurray, D. N.; Dela Cruz, E. C.; Tan, E. V.; Abalos, R. M.; Burgos, J. A.; Gelber, R.; Sakatani, M. *Vaccine* **2007**, *25*, 2990.

(33) Wheeler, L. A.; Trifonova, R.; Vrbanac, V.; Basar, E.; McKernan, S.; Xu, Z.; Seung, E.; Deruaz, M.; Dudek, T.; Einarsson, J. I; Yang, L.; Allen, T. M.; Luster, A. D.; Tager, A. M.; Dykxhoorn, D. M.; Lieberman, J. *J. Clin. Invest.* **2011**, *121*, 2401.

(34) Sundaram, P.; Kurniawan, H.; Byrne, M. E.; Wower, J. *Eur. J. Pharm. Sci.* **2013**, *48*, 259.

(35) Hamasur, B.; Haile, M.; Pawlowski, A.; Schroder, U.; Kallenius, G.; Svenson, S. B. *Clin. Exp. Immunol.* **2004**, *138*, 30.

(36) Nigou, J.; Gilleron, M.; Rojas, M.; Garcia, L. F.; Thurnher, M.; Puzo, G. *Microbes Infect.* **2002**, *4*, 945.

(37) Richmond, J. M.; Lee, J.; Green, D. S.; Kornfeld, H.; Cruikshank, W. W. *J. Immunol.* **2012**, *189*, 5886.

(38) Garg, A.; Barnes, P. F.; Roy, S.; Quiroga, M. F.; Wu, S.; Garcia, V. E.; Krutzik, S. R.; Weis, S. E.; Vankayalapati, R. *Eur. J. Immunol.* **2008**, *38*, 459.

(39) Festjens, N.; Bogaert, P.; Batni, A.; Houthuys, E.; Plets, E.; Vanderschaeghe, D.; Laukens, B.; Asselbergh, B.; Parthoens, E.; De Rycke, R.; Willart, M. A.; Jacques, P.; Elewaut, D.; Brouckaert, P.; Lambrecht, B. N.; Huygen, K.; Callewaert, N. *EMBO molecular medicine* **2011**, *3*, 222.

(40) Afonso-Barroso, A.; Clark, S. O.; Williams, A.; Rosa, G. T.; Nobrega, C.; Silva-Gomes, S.; Vale-Costa, S.; Ummels, R.; Stoker, N.; Movahedzadeh, F.; van der Ley, P.; Sloots, A.; Cot, M.; Appelmelk, B. J.; Puzo, G.; Nigou, J.; Geurtsen, J.; Appelberg, R. *Cell. Microbiol.* **2013**, *15*, 660.

(41) Geijtenbeek, T. B.; Van Vliet, S. J.; Koppel, E. A.; Sanchez-Hernandez, M.; Vandenbroucke-Grauls, C. M.; Appelmelk, B.; Van Kooyk, Y. *J. Exp. Med.* **2003**, *197*, 7.

(42) Mazurek, J.; Ignatowicz, L.; Kallenius, G.; Svenson, S. B.; Pawlowski, A.; Hamasur, B. *PLoS One* **2012**, *7*, e42515.

(43) Yonekawa, A.; Saijo, S.; Hoshino, Y.; Miyake, Y.; Ishikawa, E.; Suzukawa, M.; Inoue, H.; Tanaka, M.; Yoneyama, M.; Oh-Hora, M.; Akashi, K.; Yamasaki, S. *Immunity* **2014**, *41*, 402.

(44) Osanya, A.; Song, E. H.; Metz, K.; Shimak, R. M.; Boggiatto, P. M.; Huffman, E.; Johnson, C.; Hostetter, J. M.; Pohl, N. L.; Petersen, C. A. *Am. J. Pathol.* **2011**, *179*, 1329.

(45) Vergne, I.; Gilleron, M.; Nigou, J. *Front. Cell. Infect. Microbiol.* **2014**, *4*, 187.

(46) Zhang, C. Y.; Bai, N.; Zhang, Z. H.; Liang, N.; Dong, L.; Xiang, R.; Liu, C. H. *Cell. Mol. Immunol.* **2012**, *9*, 324.

(47) Doz, E.; Rose, S.; Court, N.; Front, S.; Vasseur, V.; Charron, S.; Gilleron, M.; Puzo, G.; Fremaux, I.; Delneste, Y.; Erard, F.; Ryffel, B.; Martin, O. R.; Quesniaux, V. F. *J. Biol. Chem.* **2009**, *284*, 23187.

(48) Zajonc, D. M.; Ainge, G. D.; Painter, G. F.; Severn, W. B.; Wilson, I. A. *J. Immunol.* **2006**, *177*, 4577.

(49) van Kooyk, Y.; Geijtenbeek, T. B. *Nat. Rev. Immunol.* **2003**, *3*, 697.

(50) Redelman-Sidi, G.; Glickman, M. S.; Bochner, B. H. *Nat. Rev. Urol.* **2014**, *11*, 153.

(51) Redelman-Sidi, G.; Iyer, G.; Solit, D. B.; Glickman, M. S. *Cancer Res.* **2013**, *73*, 1156.